Supplementary Material (ESI) for Chemical Communications


**Supplementary Information**

# Control of ZnO morphologies on carbon nanotube electrodes and electrocatalytic characteristics toward hydrazine

Kwi Nam Han, Cheng Ai Li, Minh-Phuong Ngoc Bui, Xuan-Hung Pham and Gi Hun Seong*

*Department of Bionano Engineering, Hanyang University, Ansan 425-791, South Korea.*

## Experimental Procedure

Homogeneous SWCNT films were fabricated using a vacuum filtration method. Briefly, the SWCNT mixture (Topnanosys co., South Korea) was sonicated for 1 h and then centrifuged at 14,000 rpm for ten min. The pre-suspended solution was further diluted by a factor of 50 with deionized water and filtered through an anodic aluminum oxide membrane of 0.2 μm pore size. The alumina membrane under the SWCNT thin-layer was easily removed in 3 M NaOH solution, and the SWCNT thin layer was then transferred to a flexible PET film directly after adjusting the solution to neutral pH using deionized water.

The electrodeposition of ZnO structures onto the SWCNT film was performed in a three-electrode system, in which the SWCNT film (a working electrode) was placed into a cell with a Pt wire (a counter electrode) and Ag/AgCl (saturated in 3 M NaCl) (a reference electrode). Three electrodes were put into aqueous solutions containing zinc nitrate and additives, and then a constant potential of -1.0 V (*vs.* Ag/AgCl) was applied for the fabrication of all ZnO structures in open air. Electrochemical deposition was carried out for 30 min at 70 ºC without stirring, followed by washing with deionized water and drying under nitrogen gas.

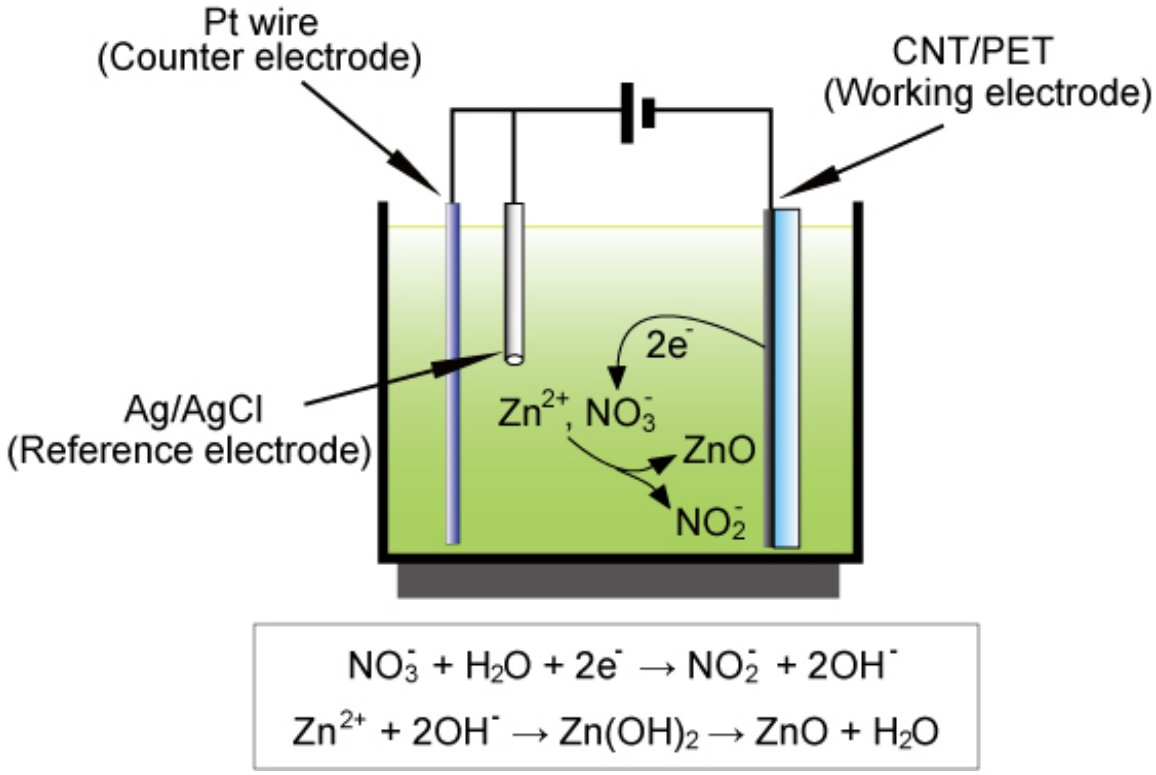


**Fig. S1** Schematic diagram for the fabrication of ZnO nanostructures on SWCNT film by electrochemical deposition.

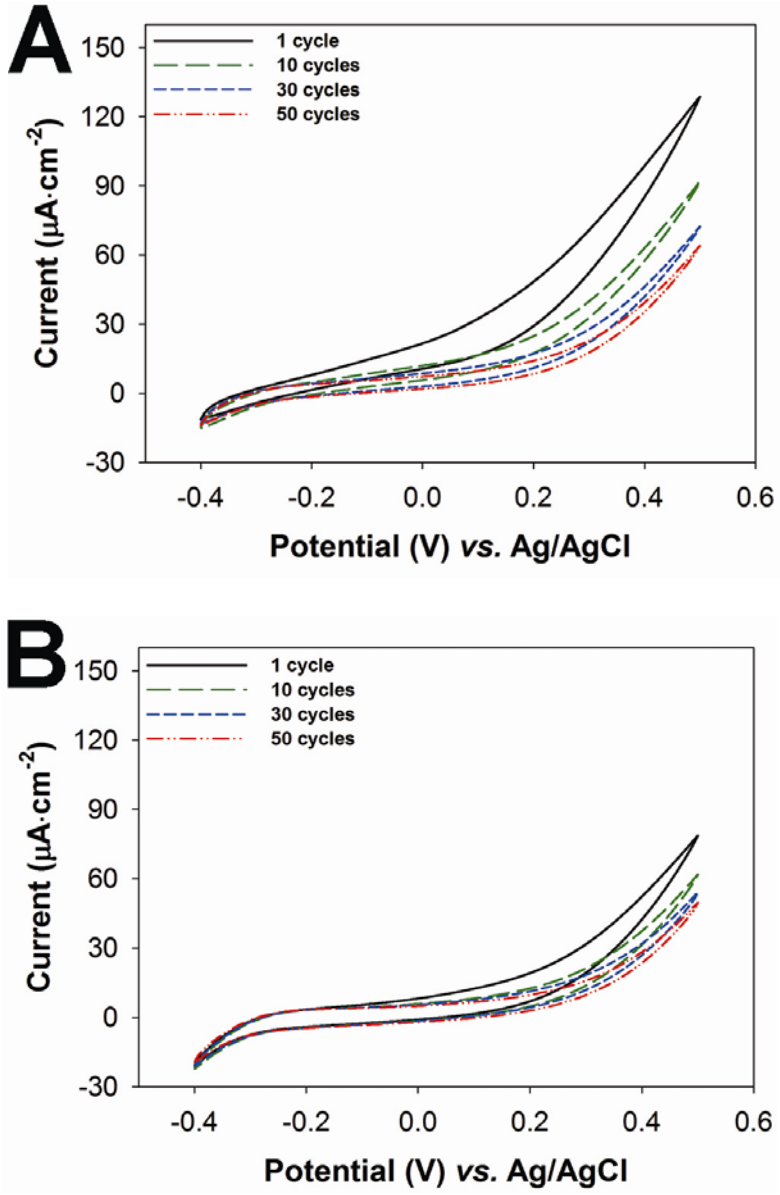


**Fig. S2** CV responses from (A) hex_particle and (B) porous sheet with increasing sweep cycles.

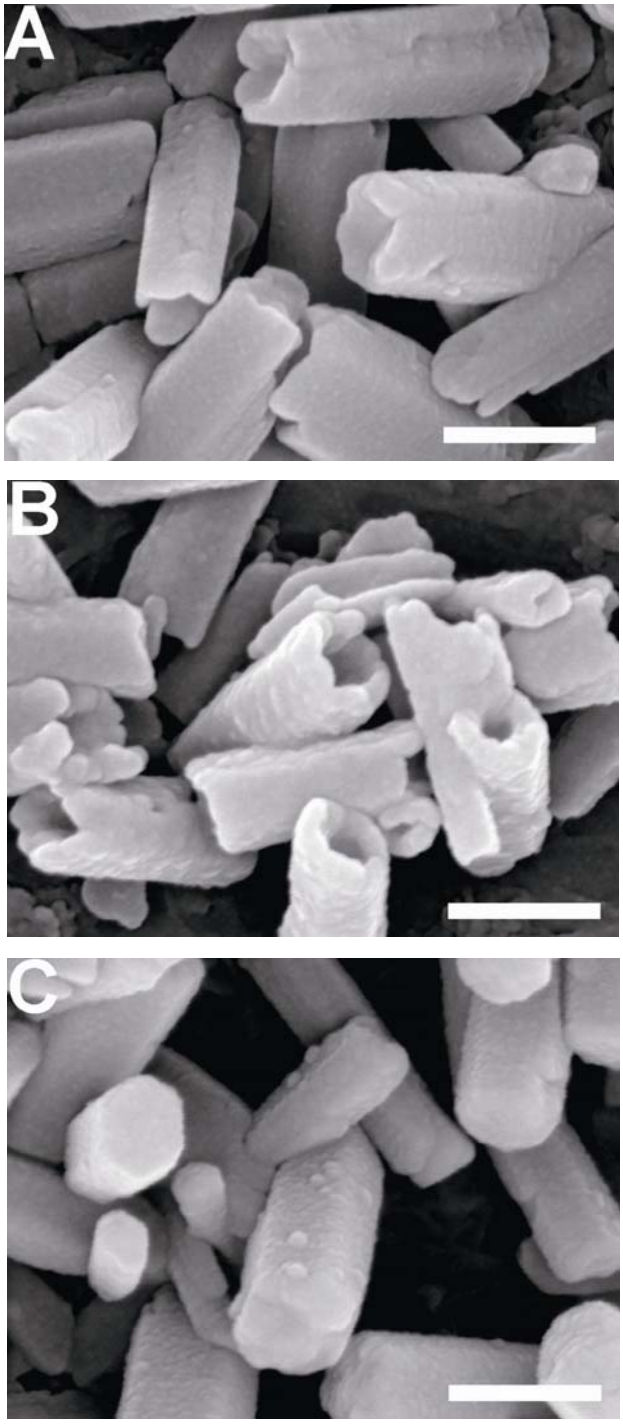


**Fig. S3** SEM images of ZnO nanorods after electro-oxidation of hydrazine using amperommetry method at constant potential of 0.2 V for (A) 30 min, and (B) 60 min. (C) SEM images of ZnO nanorods after electro-oxidation of hydrazine by cyclic voltammetry method in the potential range of -0.4 ~ 0.5 V at the scan rate of 100 mV/s for 200 cycles (60 min). The scale bars represent 300 nm.

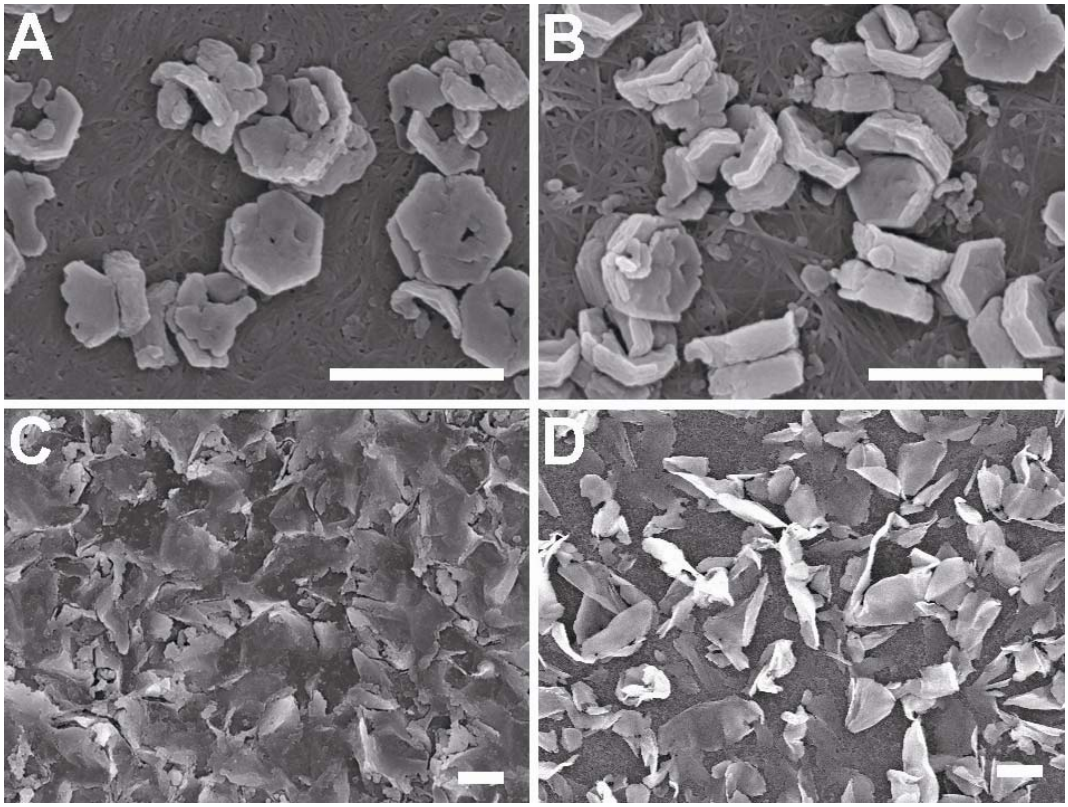


**Fig. S4** SEM images of ZnO structures after electro-oxidation of hydrazine using amperommetry method (left column) and cyclic voltammetry method (right column). (A) Hex_particles at constant potential of 0.2 V for 60 min. (B) Hex_particles in the potential range of -0.4 ~ 0.5 V at the scan rate of 100 mV/s for 200 cycles (60 min). (C) Porous sheets at constant potential of 0.2 V for 30 min. (D) Porous sheets in the potential range of -0.4 ~ 0.5 V at the scan rate of 100 mV/s for 100 cycles (30 min). The scale bars represent 500 nm in (A), (B) and 1 μm in (C), (D).

Fig. S4 shows morphological changes in hex_particle and porous sheet structures after electro-oxidation of hydrazine using amperommetry method and cyclic voltammetry method. The ZnO nanorods in Fig. S3(C) appeared to be slightly damaged after performing carrying out the electro-oxidation of hydrazine by cyclic voltammetry method. However, both ZnO hex_particle and porous sheet structures showed the distinct morphological changes after electro-oxidation of hydrazine using amperommetry method and cyclic voltammetry method.

We believe that electro-oxidation of hydrazine by cyclic voltammetry method leads to the destruction of ZnO hex_particle and porous sheet structures because hydrogen desorption is not derived from the CVs during the backward scan as shown in Fig. S2.

**Table S1** Comparison of electrocatalytic characteristics of the fabricated ZnO structures for hydrazine determination.

| **ZnO structures** | **Sensitivity ($\mu A \mu M^{-1} cm^{-2}$)** | **Detection limit ($\mu M$)** | **Response time (s)** | **Correlation coefficient ($R^2$)** |
|---|---|---|---|---|
| **Nanorod** | 0.101 | 0.170 | < 5 | 0.997 |
| **Hex_patricle** | 0.010 | 1.628 | < 5 | 0.998 |
| **Porous sheet** | 0.006 | 2.998 | < 5 | 0.994 |